

# Fast Harmonic compensation in hybrid HVDC offshore system

Shangen Tian<sup>1</sup>, David Campos-Gaona<sup>1</sup>, Rafeal Pena-Alzola<sup>1</sup> and Olimpo Anaya-Lara<sup>1</sup>

<sup>1</sup> Department of Electronic and Electrical Engineering, University of Strathclyde, Glasgow, G1 1XW, UK.

E-mail: shangen.tian@strath.ac.uk

**Abstract.** Hybrid HVDC systems have been proposed as an alternative for nominal VSC-Based HVDC for offshore applications. Hybrid HVDC systems consist of an offshore power station composed of the connection of high-power diode rectifiers in series with a fractional power VSC-HVDC. This hybrid configuration allows large power transfer from offshore sites, with the added robustness, simplicity and efficiency of uncontrolled rectifiers. In this research, a robust and fast-acting controller, the Two Degrees of Freedom Internal Model controller (2DF-IMC), is used to control the active power filter features of the fractional-power VSC-HVDC system, resulting in a much faster overall THD reduction in the offshore AC currents in dynamic conditions (i.e. time-varying wind power) when compared with standard active power filter controllers. This improvement is the direct consequence of the fast closed-loop dynamics of the 2DF-IMC controller that do not require filtering stages. Additionally, the increased closed-loop response time did not affect the overall robustness of the control system, thanks to the enhanced disturbance rejection capabilities of the 2DF-IMC configuration.

## 1. Introduction

Carbon emission reduction has become of primary importance to reduce global warming. In this regard, the United Kingdom and European Union have agreed to reduce carbon emissions to a large degree in the coming years [1], [2]. With this trend, renewable energy has become essential to meet the committed CO<sub>2</sub> reduction targets. Wind energy is the most widely used renewable energy. Compared to onshore wind energy, offshore wind provides several advantages, such as more powerful wind resources and no land occupation. However, large offshore wind farms located at long distances from shore may require high voltage direct current (HVDC) over the high voltage alternating current (HVAC) to transmit power.

Several HVDC technologies have been proposed for offshore wind farms, including line-commutated converter based HVDC (LCC-HVDC) system and voltage source converter based HVDC (VSC-HVDC) system. LCC-HVDC is the mature technology to transmit power; however, the LCC-HVDC technology requires a strong AC grid and static synchronous compensators (STATCOMs) at the point common coupling point (PCC) to support reactive power and voltage [3]. On the other hand, VSC-HVDC has a more robust control ability to manage the grid voltages and currents. For the case of offshore wind farm conditions, the VSC-HVDC can define the PCC voltage and its reactive power flow [4].

To reduce cost and install space, the diode rectifier based HVDC (DR-HVDC) system has been investigated by some researchers. The DR-HVDC uses 12 pulse diode rectifier (12-PDR) at the offshore



converter station. Since the DR technology is cheaper than VSC-HVDC, the DR-HVDC is a cost-efficiency approach for an offshore wind farm. In addition, the DR is an uncontrollable device, no need complex control system for offshore converter stations. However, a disadvantage of the DR-HVDC system is the need for WTs controllers to form the offshore grid and the requirement of a larger AC filter to cancel harmonics current at PCC point [5].

To combine the advantage of DR and VSC, the hybrid converter based HVDC system is proposed by [6]. A 12P-DR series connects with a 2-level VSC converter at an offshore converter station, the VSC controls its DC-link voltage to regulate the power share between 12P-DR and VSC in the offshore station as well as the offshore PCC voltage magnitude. In addition, the VSC is operated as an active power filter to suppress the harmonic current caused by 12P-DR. The harmonic compensation control loop uses the proportional-resonant (PR) controller[7],[8]. However, PR-control is not easy to tune, and it is susceptible to parameter variations. The reference [9] provides a simple harmonic current compensation based on PI controllers and synchronous reference frames. Although the PI controller is easy to tune, the response time is longer than the proportional-resonant (PR) controllers since it uses slow digital filtering stages for each harmonic controller. In this paper, the Two Degrees of Freedom Internal Model controller (2DF-IMC) is used to control the active power filter features of the hybrid HVDC system for a much faster response in harmonics compensation. To evidence the benefits of the proposed solution, this paper first introduces in section 2 the offshore hybrid HVDC system based on VSCs and 6-pulse diode rectifiers, including their control control system, latter on the 2DF-IMC methodology is presented. Section 3 shows the simulation results and finally, section 4 shows the conclusion of this work.

## 2. The offshore HVDC system based on VSC-6PDR hybrid Converter

### 2.1. The hybrid-HVDC configuration

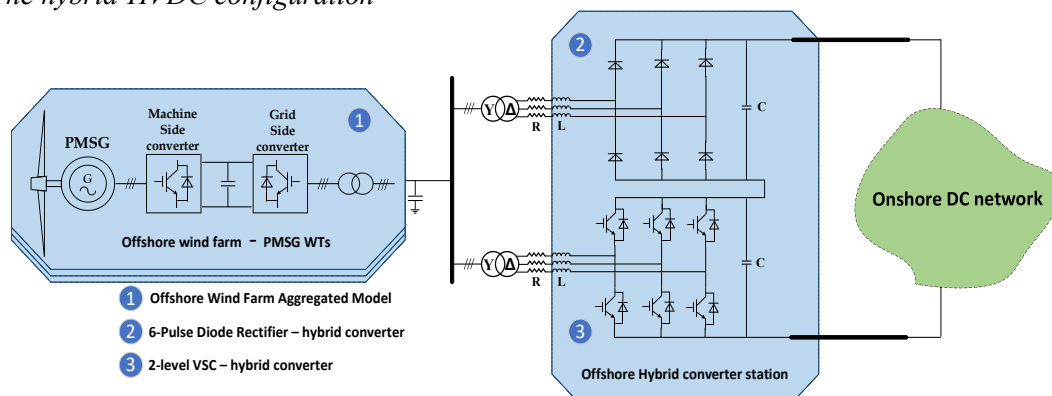
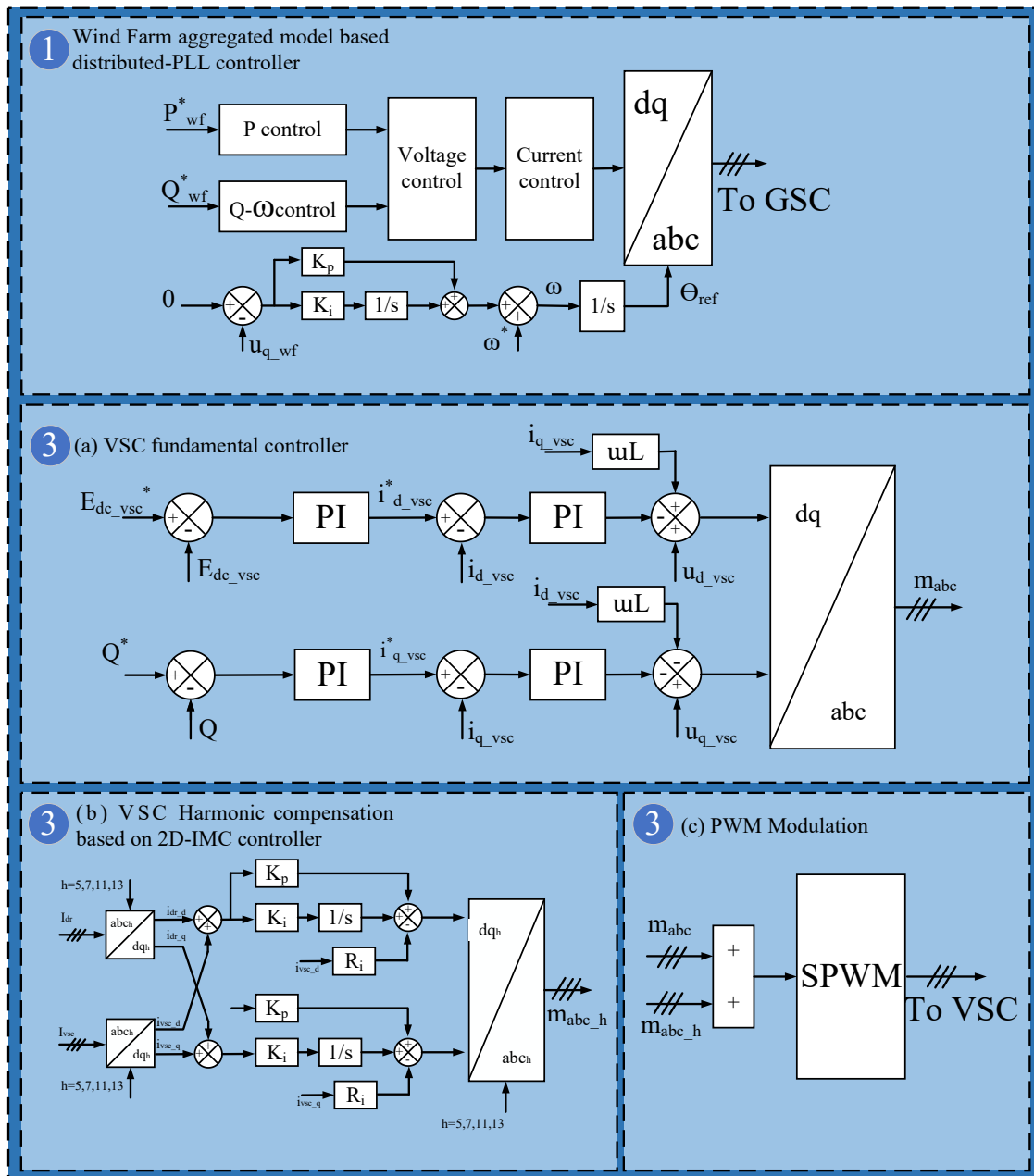


Figure 1. Offshore Hybrid-HVDC system configuration

Figure 1. shows the overall scheme of offshore HVDC system based on the hybrid converter consisting in 6P-DR in series with a 2-level VSC. The offshore converter station connects with an offshore wind farm composed of permanent magnet synchronous generator wind turbines (PMSG-WTs). The DC side of the offshore converter station is connected with the onshore HVDC converter. In this configuration, the onshore HVDC converter regulates the overall DC-link voltage of HVDC system. The offshore converter station combines the uncontrollable 6P-DR and a controllable VSC, to transmit the energy generated by the offshore wind farm. Additionally, the VSC converter inside in hybrid converter determines the power share between the 6P-DR and VSC by regulating its internal DC-capacitor voltage.



**Figure 2.** Offshore Hybrid HVDC Control System, (1) Wind Farm aggregated model controlled by distributed-PLL, (3a) Hybrid converter first harmonic controller, DC voltage controller, (3b) harmonics compensation controller based on 2D-IMC controller, (3c) PWM Modulation

## 2.2. Control system of offshore hybrid HVDC system

### 2.2.1. Control system of Offshore wind farm

An aggregated model of the PMSG-WTs, is used in this studies [10]. The control system is shown in Figure 2.(1), is a type of grid-forming converter where the active power controller and reactive power controller are used in synchrony to regulate the flows of voltage and power at the PCC point. In this proposed control system, the voltage magnitude is regulated by d-axis, the  $u_{q\_wf}$  set as 0, and as input to

maintain the frequency output to control  $u_{q\_wvf}$  equal to zero in q-axis. The relationship between  $u_{q\_wvf}$  and  $\omega$  shows below.

$$\omega = \omega_0 + K_p u_{q\_wvf} + K_i \int u_{q\_wvf} dt \quad (1)$$

$$U_{q\_wvf}^* = K_p (\omega_0 - \omega) \quad (2)$$

In this control system, the GSC in PMSG functions as grid forming converter to form the AC voltage at PCC point, the distributed PLL regulated the frequency. The outer controller is controlling the active power and reactive power to offshore converter station. The distributed-PLL controller is first proposed in DR-HVDC, more details is described in [10].

### 2.2.2. First harmonics control system

The onshore DC networks regulate the overall DC voltage of HVDC system. Since the diode rectifier is an uncontrollable converter, the VSC converter controls the offshore hybrid converter to transmit power. The overall control system is shown in Figure 2(3). In this series connection configuration, the transmitted power is proportional to its DC-link voltage. The inner current control has been widely used in VSC control to provide fast response and current limit. The inner current relationship is shown below.

$$u_{conv\_d} = i_{d\_vsc} R + L \frac{di_{d\_vsc}}{dt} + u_{d\_vsc} - \omega L i_{q\_vsc} \quad (3)$$

$$u_{conv\_q} = i_{q\_vsc} R + L \frac{di_{q\_vsc}}{dt} + u_{q\_vsc} + \omega L i_{d\_vsc} \quad (4)$$

As the mentioned before, the DC-link voltage of converters is proportional to its transmitted power, the outer controller of VSC in hybrid converter station chosen as DC voltage controller in d-axis, the q-axis can be controlled as reactive power controller to control the reactive power magnitude to support. the equation (5) shows the DC voltage controller mathematical model.

$$i_{d\_vsc} = K_{p\_dc} (E_{vsc\_dc}^* - E_{dc}) + K_{i\_dc} \int E_{vsc\_dc}^* - E_{dc} dt \quad (5)$$

Additionally, the equation (6) shows the relationship between PCC point and  $dq$  current.

$$q(t) = \frac{3}{2} [-v_{d\_vsc}(t) i_{q\_vsc}(t) + v_{q\_vsc}(t) i_{d\_vsc}(t)] \quad (6)$$

In addition to DC voltage controller and reactive power controllers in first harmonics control loop, the 5<sup>th</sup>, 7<sup>th</sup>, 11<sup>th</sup> and 13<sup>th</sup> harmonic current compensation are included in the VSC control system. The next section introduces the harmonic current compensation controller.

### 2.2.3. Harmonic current compensation control

Due to the hybrid converter topology, the 6-PDR introduces many harmonics currents into PCC point. The VSC control in the hybrid converter functions as an active power filter to cancel out the harmonic currents. In [6], the 12-PDR used for the hybrid converter included a *YYD* transformer. In such transformer, the secondary side phase angle reduces 5<sup>th</sup> and 7<sup>th</sup> harmonic currents while the rest of the harmonic current compensation is carried out using PR-controller. The YD transformer and 6-PDR are used in this study to reduce the cost and complex transformer structure. The two techniques for harmonic cancellation are described below.

The PR-controller can follow the sinusoidal harmonic current references at their separated resonant frequencies. No steady-state error occurs when applying the infinite gain at respective resonant frequency. In addition, PR-controller has fast response time for a setpoint change. However, the complex process of system stability tuning is a disadvantage of PR-controller. In addition, this control process is susceptible to changes in grid frequency because of the narrow high-gain band for each harmonic. The second-order generalized integrators used in non-ideal PR-controller leading to wider resonant band which increases tracking error [11].

Another technique is the synchronous reference frame (SRF)-based controller, which used PI controller to provide an easy-to-tune method to control the singles without tracking errors [12]. However,

slow harmonics detection and compensation is a problem for SRF-based controllers. To evidences the Section 2.2.3.1 and 2.2.3.2 introduces the SRF-controller with its internal low pass filter proposes the SRF-controller based on the 2D-IMC controller architecture.

### 2.2.3.1 SRF controller with low pass filter

In SRF-controller, several synchronous  $dq$  reference frames rotate the frequency and sequence of individual harmonic currents. For example, the synchronous  $dq$  reference frame rotating at 5<sup>th</sup> times the fundamental can obtain a  $dq$  value of the 5<sup>th</sup> harmonics current. The output of the  $dq$  transformation produces an AC-signals plus the DC-signals. The DC-signals represent the  $h$  harmonic currents of the  $h$ -rotating  $dq$  frame. The output of the rotating  $dq$  frame is filtered by low-pass filter to isolate the DC signals from the rest of the harmonics and then provided to the PI controller. Figure 3. shows the block diagram of SRF-harmonics compensation based on PI controller with a low-pass filter. Since the VSC AC output is connected in parallel to the DR, the harmonic current at PCC point can be cancelled out by the VSC harmonic controller. However, the low pass filter in the SRF-PI control structure delays harmonic detection and mitigation. Additionally, including low-pass filters increases the computational burden of the control system [12].

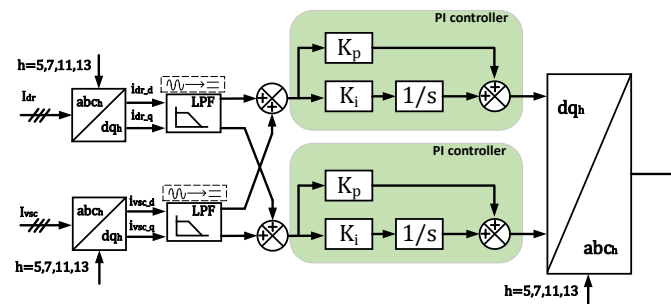


Figure 3. SRF-harmonics compensation based on PI controller

### 2.2.3.2 Harmonics compensation with 2DF-IMC

To reduce the delay of the low-pass filter, the two-degrees-of-freedom replacing the PI controller in SRF harmonics compensation process is proposed. By this replacement, the 2DF-IMC of each individual harmonic current compensation loops would track the harmonics at set-point at the same time without delay [13]. Figure 5. shows the structure of the IMC controller modified to graphically group the controller section and the plant section in the closed loop system. Also, Figure 5 includes the representation of an inner feedback loop of gain  $R$  in the plant, which is designed to provide an extra (a second) degree of control freedom (2DF). This additional degree of control is used to speed up the natural response of the plant by moving the pole of the plant away from the origin within the negative side of the real axis. The additional degree of control freedom greatly improves the load disturbance rejection characteristic of the plant which, by itself, is independent of the set-point tracking controller.

The load disturbance rejection feature of the 2DF-IMC is specifically designed to reject DC disturbances with 0 steady state error. This feature is the key factor for the filter-less realization of a SRF controller since, as it will be explained below, the negative effects of removing the low pass filters from the conventional SRF control structure is a control loop polluted with AC harmonic signals. Nevertheless the 2DF-IMC is able to dealt-with this harmonic pollution in the DC domain.

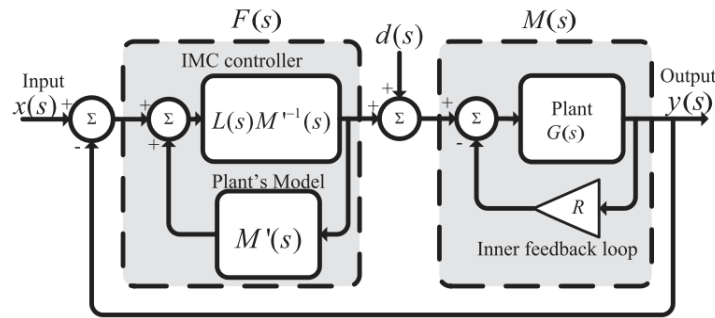


Figure 4 The diagram of IMC controller [13]

The application of a  $dq0$  harmonic transformation  $T_n$  to a 3 phase current signal with harmonic content would produce, as an output, a  $dq0$  signal comprising the DC  $dq$  components of the  $n$  harmonic, plus an AC component, with the rest of the harmonics moved in frequency, depending on the sequence of the  $n$  harmonic and the sequence of the rest of the harmonics. Mathematically this is:

$$i_{n,d} = \underbrace{\Gamma_n i_n \cos(\beta_n)}_{\text{DC component}} + \underbrace{\sum_{k=1, k \neq n}^{\infty} \Gamma_k i_k \cos(-\Gamma_k [(\Gamma_n n - \Gamma_k k)(\omega_s t)] + \beta_k)}_{\text{AC component}} \quad (7)$$

$$i_{n,q} = \underbrace{i_n \sin(\beta_n)}_{\text{DC component}} + \underbrace{\sum_{k=1, k \neq n}^{\infty} i_k \sin(-\Gamma_k [(\Gamma_n n - \Gamma_k k)(\omega_s t)] + \beta_k)}_{\text{AC component}}$$

where  $i_{n,d}$  and  $i_{n,q}$  are the  $n$  harmonic  $dq$  signals respectively.  $\beta_n$  is the phase shift of the  $n$  harmonic,  $i_n$  is the magnitude of the  $n$  harmonic,  $i_k$  is the magnitude of the  $k$  harmonic current,  $\omega_s$  is the synchronous frequency in radians,  $t$  is the time,  $\beta_k$  is the phase shift of the  $k$  harmonic, and  $\Gamma_k = \text{sign}[\sin(2\pi k/3)]$  represents the sequence of the  $k$  harmonic and is reflected in (7) as an algebraic sign.

If the AC components of the  $dq$  currents in (7) are allowed to propagate in the control loops then the controller output will become a hybrid signal composed of a DC part (the useful control action) plus a AC part (the AC harmonic pollution). This applies to any AC harmonic signal fed to the 2DF-IMC. The 2DF-IMC AC output components would add up and, together, would be processed by the inverse transformation  $T_n^{-1}$ , eventually being fed as modulator signals to the VSC.

The the modulator signal fed to the VSC by a filter-less SRF is a hybrid waveform composed of 2 parts: 1) A useful control action (the DC dynamics of the fundamental and harmonic  $dq$  current loops) plus 2) constant harmonic disturbances (product of using filter-less SRF) which are meaningless for control purposes. However, these AC disturbances can be fully rejected in the DC domain with 0 steady state error when using 2DF-IMC.

The constant AC harmonic disturbances produced by the filter-less 2DF-IMC are innocuous for a selective harmonic compensator based on the 2DF-IMC. The reason for this is that a  $n$  constant AC harmonic disturbance, produced by any given 2DF-IMC controller of the system, is reflected as a constant DC signal disturbance in the 2DF-IMC dedicated to the control of the  $n$  harmonic (specifically, it will be reflected as a DC disturbance signal of magnitude  $H_{n,AC} \cos(\beta_n - \phi_{n,AC})$  for the  $d$  control loop, and a DC disturbance signal of magnitude  $H_{n,AC} \sin(\beta_n - \phi_{n,AC})$  for the  $q$  control loop.

Since the 2DF-IMC is specifically designed to reject step-like and constant DC disturbances, is an ideal fit to compensate the AC disturbances produced by the other 2DF-IMC controllers with the same robustness and speed of response of its set-point tracking characteristics, since they will be reflected as a DC disturbance signal. Because of this, an array of 2DF-IMCs dedicated to compensating individual harmonics, will collectively compensate the AC disturbances produced by one another as fast as they

track a set point change. A schematic diagram of the 2DF-IMC along with the SRF is shown in Figure 5.

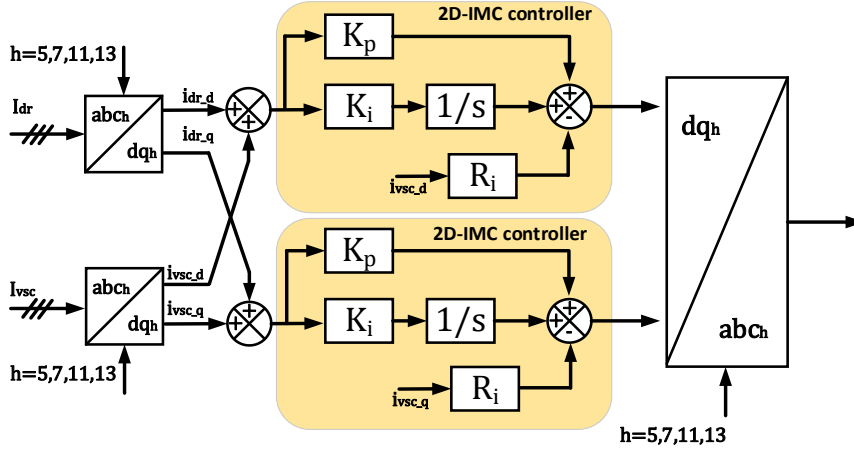


Figure 5. Harmonics compensation based on 2DF-IMC controller

The tuning of the controller constants of the system is as follows. The equations defining the dynamics of the  $d$ - $q$  fundamental and harmonic currents between the VSC and the AC grid are:

$$v_{n,d\_inv} = r i_{n,d} + l di_{n,d}/dt - \omega_s l i_{n,q} - v_d \tag{8}$$

$$v_{n,q\_inv} = r i_{n,q} + l di_{n,q}/dt + \omega_s l i_{n,d} - v_q$$

where  $r$  and  $l$  are, respectively, the equivalent resistance and inductance between the VSC and the AC grid,  $i_{n,d}$  and  $i_{n,q}$  are the average  $dq$  current components of the  $n$  harmonic,  $v_{n,d\_inv}$  and  $v_{n,q\_inv}$  are the  $dq$  components of the  $n$  harmonic of the average voltages generated by the VSC and where  $v_d$  and  $v_q$  are the  $dq$  voltage components of the offshore AC grid.

The transfer functions between  $dq$  VSC harmonic currents and the  $dq$  VSC harmonic voltages can be represented by the same equation if the cross-coupling terms ( $\omega_s l i_{n,q}$  and  $\omega_s l i_{n,d}$ ), and the grid voltage components, ( $v_d$  and  $v_q$ ) from (8) are considered disturbances, not present during the calculation of the  $dq$  current control, but instead being numerically compensated by a feedforward loop. Hence, the VSC current-to-voltage relationships in the  $dq$  frame is given by

$$\frac{i_{n,d}(s)}{v_{n,d\_inv}(s)} = \frac{i_{n,q}(s)}{v_{n,q\_inv}(s)} = \frac{i_n(s)}{v_{n\_inv}(s)} = G_i(s) = \frac{1}{ls + r} \tag{9}$$

If an inner feedback loop of gain  $R_i$  is added to  $G_i$  (i.e a second degree of control freedom an enhanced transfer function of the following type is obtained:

$$M_i(s) = 1/(R_i + ls + r) \tag{10}$$

The inner feedback loop is implemented in the plant by making the input signal to the plant equal to

$$v_{n\_inv}(s) = v_{n\_inv}'(s) - i_n(s)R_i \tag{11}$$

Under this scenario the 2DF-IMC control constants are

$$Kp_i = \alpha_i l \quad Ki_i = (r + R_i)\alpha_i \tag{12}$$

Where  $\alpha_i$  is the bandwidth of the closed loop system and is selected based in the speed of response of the controllers. If the gain of  $R_i$  is selected to match the pole of  $M_i(s)$  with the pole of  $F_i(s)$  on the transfer function from the disturbance  $d_i(s)$  to the output of the plant, then  $R_i$  is required to have the value of

$$R_i = \alpha_i l - r \tag{13}$$

With a value of  $R_i$  specified by (13) the relationship between output voltage and disturbances  $v_{n\_inv}(s)/d_{n,i}(s)$  becomes

$$v_{n\_inv}(s)/d_i(s) = s/(l(\alpha_i + s)^2) \tag{14}$$



As seen in (14), the disturbances  $d_i(s)$  are rejected by the plant and the controller with the same time constant, which in turn depends on  $\alpha_i$ .

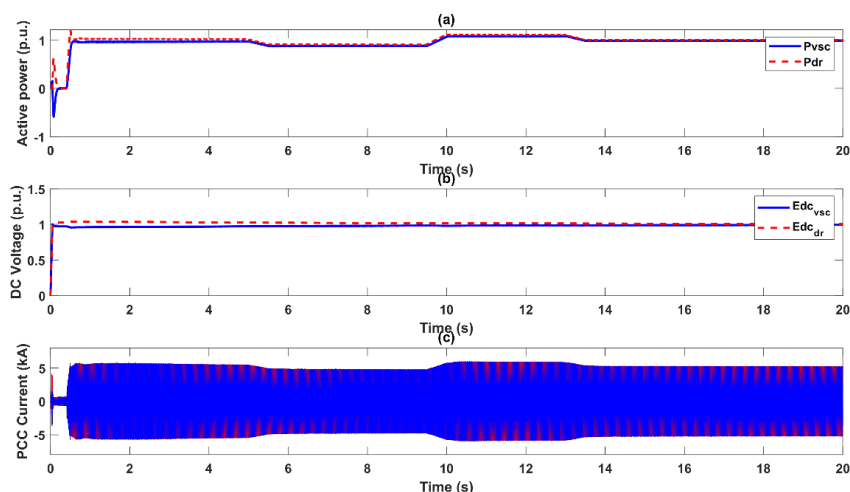
### 3. Simulation results

The hybrid HVDC system is built in PSCAD to verify the HVDC system operated as varying wind turbine input active power and the harmonics current compensation by 2DF-IMC controller. The parameters used in PSCAD model is shown in Table 1.

**Table 1** The parameters of hybrid HVDC system

| Components                                  | Parameters             | Nonmail value |
|---|------------------------|---------------|
| Wind turbine                                | Active power           | 400 MW        |
|   | Transformer ratio(Y/D) | 0.69/66 kV    |
| 6 Pulse Diode Rectifier Of Hybrid converter | Transformer ratio(Y/D) | 66/123 kV     |
|   | Resistance             | 0.0139 ohm    |
|   | Inductance             | 0.0172 H      |
|   | DC voltage             | 160 kV        |
|   | Active power           | 200 MW        |
|   | Transformer ratio(Y/D) | 66/123 kV     |
| 2-Level VSC Of Hybrid converter             | Resistance             | 0.0139 ohm    |
|   | Inductance             | 0.0172 H      |
|   | DC voltage             | 160 kV        |
|   | Active power           | 200 MW        |
|   | Transformer ratio(Y/D) | 66/123 kV     |

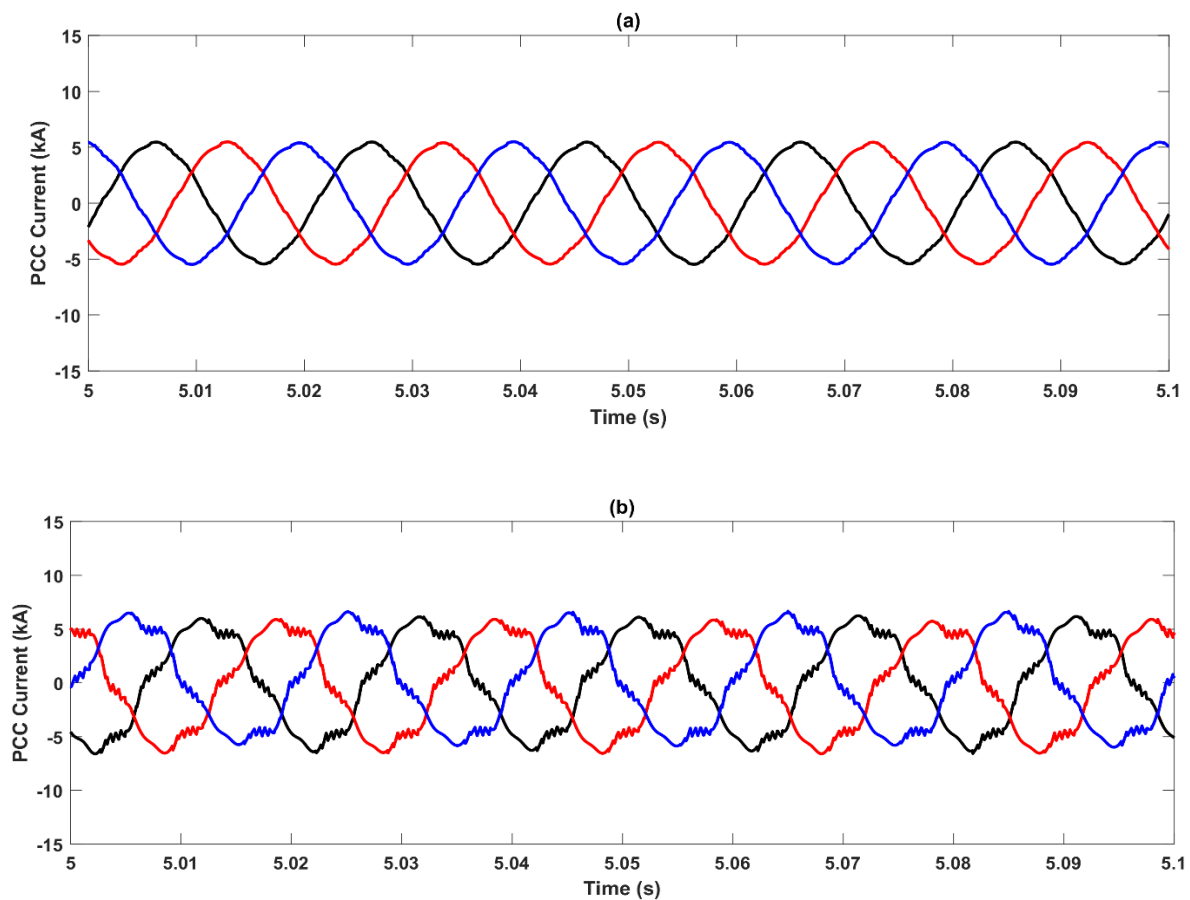
Figure 6 shows the simulation results on the hybrid converter operate at different wind turbine input power steps. The VSC control the DC link voltage as 160 kV (1 p.u.) and the DC link voltage of diode rectifier is rest of overall HVDC system DC link voltage that is 160 kV (1 p.u.). Due to the series connection of hybrid converter station, the two components of hybrid converter is proportional to its DC link voltage. which the Figure 6 (a) shows the active power of hybrid converter transmit equal demand active power because converter of hybrid converter is controlled in the same share in hybrid HVDC system.



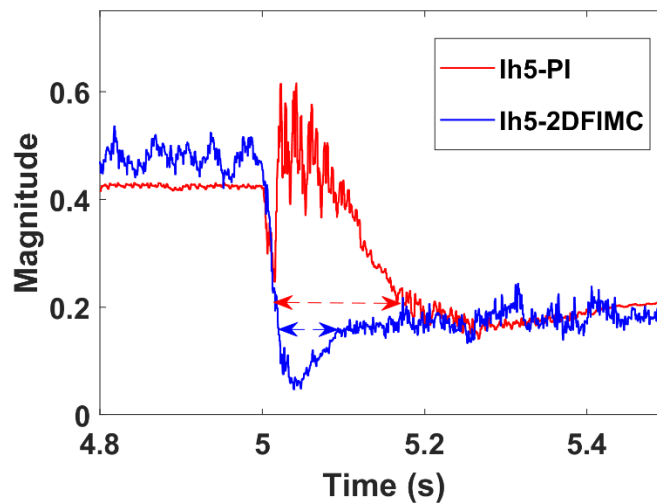
**Figure 6** Performance of hybrid HVDC system based on 6-PD and VSC, (a) transmitted active power of hybrid converter components; (b) DC-link voltage of hybrid converter components; (c) Current at PCC point.



Figure 7 shows the different case of hybrid HVDC system that when the 2DF-IMC controller enabled and disabled. Figure 7 (a) shows the current at PCC point when the built-in active power filter enabled which the VSC of hybrid converter control by SRF harmonics compensation control loop used 2DF-IMC controller and Figure 7 (b) display the shape of PCC current when harmonics compensation controller disabled. In addition, in order to show the response time of harmonics compensation, the 5<sup>th</sup> and 7<sup>th</sup> harmonics compensation response time is show in Figure 8. The hybrid converter work at no harmonics compensation at the beginning, at 5s, the harmonics compensation control started to work and the VSC converter functions as an active power filter to cancel out the selective harmonics current.



**Figure 7** The current waveform at PCC point, (a) PCC current – harmonics compensation operated  
(b) PCC current – harmonics compensation disabled



**Figure 8** The comparison of 5<sup>th</sup> harmonic current compensated by PI and 2DFIMC

#### 4. Conclusion

The HVDC system based on hybrid converters used for offshore wind power is discussed in this paper. Furthermore, the proposed control system and harmonics current compensation controller is also introduced. The hybrid converter combines two kinds of power electronics converter in the proposed system, 6-pulse diode rectifier and a VSC converter. The VSC converter controls its DC link voltage. Therefore, the transmitted active power is proportional to DC voltage. In addition, the VSC of a hybrid converter works as an active power filter to remove the requirements of passive filtering devices.

This paper discusses the harmonics compensation controllers using PI control or 2DF-IMC controller in detail. The harmonics compensation controller is based on SRF technique to detect selective harmonics current. If PI controllers are used for the active power filtering, a low pass filter stage that decreases the system's response time needs to be used. However, the two-freedom degree internal model controller replaces PI controller in the harmonics compensation controller in this work. In this configuration, no filtering stages are required. This increases the closed-loop response time of the system and provides a more attractive option for the deployment of hybrid offshore systems.

To offshore hybrid converter, the power electronic device choice, the size of component and black start strategy can be future improved. The different converter components provide its highlight to hybrid converter, as the hybrid converter aims to combine their advantages, for example, MMC converter can instead of VSC converter, which controls DC voltage and brings a better protection ability to hybrid converter. In addition, hybrid converter can future reduce the cost though increasing the size of diode rectifier, and the rest of controllable device can be controlled as an active power filter to cancel out the harmonic current at PCC point. Finding a transmitted power ratio (by controlling dc voltage) to ensure hybrid converter can work in high performance and cost-effective.

#### References

- [1] UK Government, "UK becomes first major economy to pass net zero emissions law," *Department for Business, Energy & Industrial Strategy*. 2019, [Online]. Available: <https://www.gov.uk/government/news/uk-becomes-first-major-economy-to-pass-net-zero-emissions-law>.
- [2] European Commission, "A European Green Deal | European Commission," *European Commission*. p. 24, 2019, [Online]. Available: <https://ec.europa.eu/info/strategy/priorities->

- 2019-2024/european-green-deal\_en.
- [3] R. Li, S. V. Bozhko, and G. M. Asher, "Grid frequency control for LCC HVDC link connected wind farms," *IECON Proc. (Industrial Electron. Conf.)*, pp. 1673–1678, 2007, doi: 10.1109/IECON.2007.4460235.
- [4] A. Korompili, Q. Wu, and H. Zhao, "Review of VSC HVDC connection for offshore wind power integration," *Renew. Sustain. Energy Rev.*, vol. 59, pp. 1405–1414, 2016, doi: 10.1016/j.rser.2016.01.064.
- [5] R. Blasco-Gimenez, S. Añó-Villalba, J. Rodríguez-D'Herlée, F. Morant, and S. Bernal-Perez, "Distributed voltage and frequency control of offshore wind farms connected with a diode-based HVdc link," *IEEE Trans. Power Electron.*, vol. 25, no. 12, pp. 3095–3105, 2010, doi: 10.1109/TPEL.2010.2086491.
- [6] T. H. Nguyen, D. C. Lee, and C. K. Kim, "A series-connected topology of a diode rectifier and a voltage-source converter for an HVDC transmission system," *IEEE Trans. Power Electron.*, vol. 29, no. 4, pp. 1579–1584, 2014, doi: 10.1109/TPEL.2013.2283368.
- [7] A. Uphues, K. Notzold, R. Wegener, and S. Soter, "Frequency adaptive PR-controller for compensation of current harmonics," *IECON Proc. (Industrial Electron. Conf.)*, pp. 2103–2108, 2014, doi: 10.1109/IECON.2014.7048792.
- [8] L. Yang, C. Xiong, Y. Teng, Q. Hui, and Y. Zhu, "Harmonic Current Suppression of Grid-Connected PV Based on PR Control Strategy," *Proc. - 2015 6th Int. Conf. Intell. Syst. Des. Eng. Appl. ISDEA 2015*, pp. 433–436, 2016, doi: 10.1109/ISDEA.2015.114.
- [9] S. Tian, D. Campos-gaona, A. Lacerda, R. E. Torres-olguin, and O. Anaya-lara, "Novel Control Approach for a Hybrid Grid-Forming HVDC Offshore Transmission System," pp. 1–14, 2020.
- [10] L. Yu, R. Li, and L. Xu, "Distributed PLL-based Control of Offshore Wind Turbine Connected with Diode-Rectifier based HVDC Systems," *IEEE Trans. Power Deliv.*, 2017, doi: 10.1109/TPWRD.2017.2772342.
- [11] L. Herman, I. Papic, and B. Blazic, "A proportional-resonant current controller for selective harmonic compensation in a hybrid active power filter," *IEEE Trans. Power Deliv.*, vol. 29, no. 5, pp. 2055–2065, 2014, doi: 10.1109/TPWRD.2014.2344770.
- [12] J. L. M. Morales, M. H. Ángeles, D. Campos-Gaona, and R. Peña-Alzola, "Control design of a neutral point clamped converter based active power filter for the selective harmonic compensation," *2016 IEEE PES Transm. Distrib. Conf. Expo. Am. PES T D-LA 2016*, 2017, doi: 10.1109/TDC-LA.2016.7805687.
- [13] D. Campos-Gaona, R. Pena-Alzola, J. L. Monroy-Morales, M. Ordonez, O. Anaya-Lara, and W. E. Leithead, "Fast selective harmonic mitigation in multifunctional inverters using internal model controllers and synchronous reference frames," *IEEE Trans. Ind. Electron.*, vol. 64, no. 8, pp. 6338–6349, 2017, doi: 10.1109/TIE.2017.2682003.